Longitudinal Vortex Wind Turbine: Effect of the Blade Lengths

W. Hemsuwan, K. Sakamoto and T. Takahashi

Abstract The longitudinal vortex wind turbine (LV-WT) is a novel propeller type, but the turbine blade is the circular cylinder. The blade is driven by lift force of the longitudinal vortex (LV). This work is to examine a simple single-cylinder blade to suppress the negative driving-force portion by cutting and keeping only the useful area. Unsteady Reynolds-Averaged Navier-Stokes (URANS) simulation is used for investigation. For the original single blade, the positive driving force was generated around the dominance of the LV at the crossing section. Meanwhile, the negative driving force appears far from the ring regime. When the original blade is diminished to avoid the unpleasant parts, the negative regions are suppressed completely. The distribution of the aerodynamic forces along the blade length is symmetric for the length extended equally. Final, the equally extended blade with the length of three times of the ring width is built and tested in the wind tunnel. The tendency of the experimental data and the CFD results correlate very well.

Keywords Wind turbine · Circular cylinder propeller · Longitudinal vortex Longitudinal vortex induced steady lift force · Wake

W. Hemsuwan
Graduate School of Engineering, Nagaoka University of Technology, Nagaoka, Niigata, Japan

K. Sakamoto
Department of Science of Technology Innovation, Nagaoka University of Technology, Nagaoka, Niigata, Japan

T. Takahashi (✉)
Department of Mechanical Engineering, Nagaoka University of Technology, Nagaoka, Niigata, Japan
e-mail: ttaka@nagaokaut.ac.jp

Y. Zhou et al. (eds.), *Fluid-Structure-Sound Interactions and Control*, Lecture Notes in Mechanical Engineering,
https://doi.org/10.1007/978-981-10-7542-1_18

1 Introduction

A newly developed innovative wind/water turbine (WT) with the circular cylinder blades driven by the longitudinal vortex has been firstly presented by [3] that was called the "*longitudinal vortex wind/water turbine: LV-WT.*" Two major components of this turbine are the circular cylinder blades and a ring-shaped plate. The photograph and schematic diagrams of this system are shown in Fig. 1. The ring plate is located behind the cylinder by retaining a suitable gap between them. The longitudinal vortex (LV) is generated at the crisscross region of the ring regime, but it is not stably existing. However, once the cylinder moves along the ring plate, the LV stably exists at the backside of the cylinder and moves with the cylinder. The driving lift force is produced steadily due to the aerodynamic effect of the LV. The mechanical structure of the LV-WT system is very simple compared with the Magnus WT, which is driven by the Magnus force of the spinning cylinders that are powered by the built-in motors for employing the Magnus effect [1] and the extra energy for spinning is also required. Whereas, it is unneeded for the LV-WT.

In this study, the original single blade will be investigated in order to avoid the negative portion. The effect of the blade lengths will be examined by using the URANS simulation.

2 Numerical Modeling

In order to investigate the effect of the blade lengths on the performance of the LV-WT, the original single cylinder blade in Fig. 1b is divided into the two blades. The parameters of the blade extension ratios l_1/W and l_2/W shown in Fig. 1c are accomplished using the URANS simulation with the moving mesh model. The numerical region is divided into the two domains, an inner circular domain and an outer rectangular domain. The inner domain encloses the cylinder blades which is defined as the moving zone, while the outer domain contains the ring plate, the tunnel walls, the inlet and outlet which is defined as the stationary. The 3D

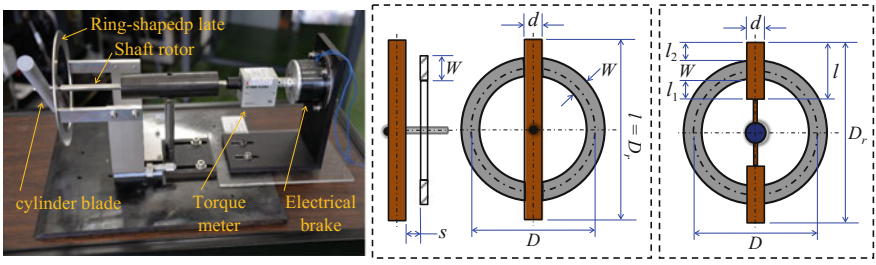

(a) Photograph of experimental apparatus (b) Single cylinder blade WT (c) Two cylinder-blades WT

Fig. 1 Photograph of experimental system and schematic diagram of the LV-WT system

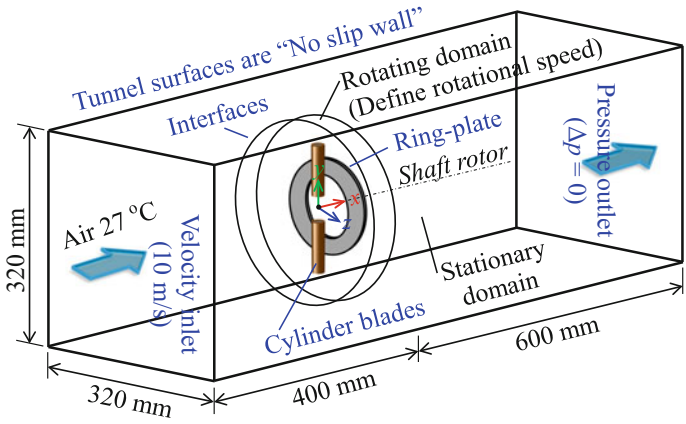

Fig. 2 Schematic diagram of numerical domains and boundary conditions setup

unstructured mesh is calculated by ANSYS-CFX 18.0 based on finite volume method. Figure 2 shows the summary of the CFD domains and boundary condition types. The validations of the mesh resolution and the turbulence model used *SST k-ω* for this calculation had been reported in the previous study [3].

All calculations are performed for the two blades LV-WT system with the free velocity $U_\infty = 10$ m/s (Re = 1.272×10^4 based on the cylinder blade diameter). The cylinder blade diameter $d = 20$ mm, the center diameter of the ring plate $D = 155$ mm, the ratio of the ring width to the blade diameter $W/d = 1$, the gap distance normalized by the blade diameter $s/d = 0.35$, and the tip speed ratio base on the length of the single cylinder blade ($l = 220$ mm) $\lambda = 0.5\omega l/U_\infty = 0.2$. The blade extension ratios l_1/W and l_2/W are varied.

3 Results and Discussion

Flow field around the cylinder blade will be visualized for understanding the aerodynamic driving force. Distribution of the fluid force along the blade length is evaluated to find the effective area in the blade. The best length for the high performance in the experimental investigation in our wind tunnel instrument will be examined, and the CFD results will be compared with the experimental data.

3.1 Flow Visualization

Figure 3 shows instantaneous flow fields around of the cylinder blade on a plane perpendicular to the cylinder axis at the middle of the ring width. The streamline

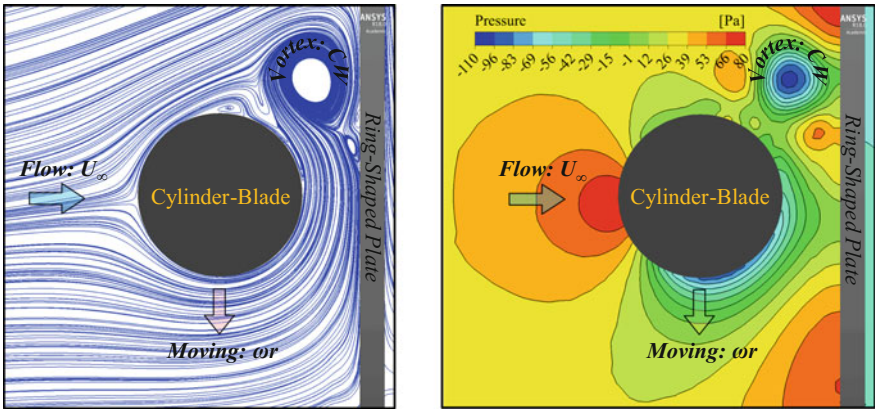

Fig. 3 Instantaneous flow visualizations of the single blade WT on cross section of the cylinder at the middle of the ring width; streamlines visualization (left) and pressure contour (right)

visualization displays a vortex (LV) behind the cylinder blade and locates between the ring plate. The vortex has the rotation direction of $\boldsymbol{Flow} \times \boldsymbol{Motion}_{\boldsymbol{cylinder}}$ (CW for this case) and appears along the cylinder length, but limited by the ring regime. The acceleration flow is found on the moving side due to the strong suction flow of the LV. The net lift force is produced in the moving direction due to the difference of pressure gradient on the cylinder surface that is the aerodynamic effects of this vortex. Outside of the LV regime is the subcritical flow, the disturbance of the wake behind the cylinder bluff body produces the drag force, the steady lift cannot be generated in this region, and it will reduce the performance of the turbine.

3.2 Force Distributions Along the Cylinder-Blade Length

The distribution of the aerodynamic force acting on the cylinder surface along the blade length is evaluated to examine the effective length of the blade. One of the cylinder blades is split into the very short segments with an equally lengthwise of $\Delta l = 0.02d$, the forces acting on each segment are evaluated by integrating the stress acting on their cylindrical surface. The components of the force coefficients on the small sectional blade i are given by; $C_{t,i} = F_{t,i}/0.5\rho A_i {U_\infty}^2$ and $C_{a,i} = F_{a,i}/0.5\rho A_i {U_\infty}^2$. Where, $F_{a,i} = F_{x,i}$ is the force in the axial direction of the rotor shaft, and $F_{t,i} = M_{x,i}/r_i$ is the force in the tangential direction of the rotor plane at rotor radius r_i. When, $M_{x,i}$ is the summation moment due to pressure and stress force, and $A_i = d\Delta l$ is the frontal area of the cylindrical segment.

The tangential and axial force coefficients; $C_{t,i}$ and $C_{a,i}$ of the small blade elements are plotted along the normalized blade length r/R as shown in Fig. 4. For the original single-blade, the values of C_t and C_a near the origin ($r/R = 0$) are similar to the subcritical flow over a stationary cylinder that is the time-averaged of $C_t = C_l =$

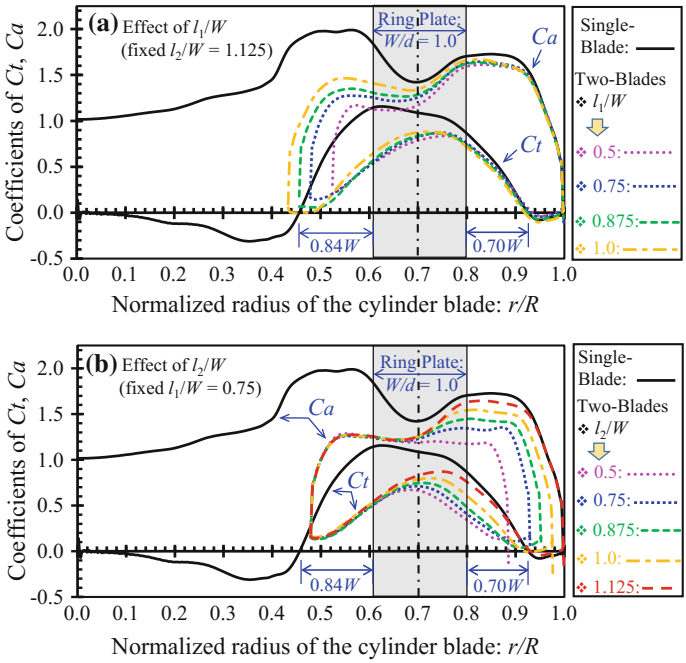

Fig. 4 Distribution of force coefficients C_t and C_a along the cylinder blade length; **a** effect of parameter l_1/W (fixed $l_2/W = 1.125$), **b** effect of parameter l_2/W (fixed $l_1/W = 0.75$)

0 and $C_a = C_d \approx 1.2$ [2]. The negative driving force appears at about $r/R = 0.1$–0.45 as seen in the distribution of C_t. This region is the subcritical flow exterior LV regime where the effective drag is produced but the steady lift cannot be generate. In this case, the negative C_t is the projected net drag from the line of attack of the relative velocity through the tangential direction of the rotor plane. The incline angle of the line of attack is zero at the origin and increases through the blade tip. Therefore, the C_t is zero at the root and strongly reduces into the negative values where increasing radius. Near the crossing region (LV regime), the positive driving force is generated by resulting of the LV (Fig. 3), and decreases again near the tip tends to be the negative values when the top length is extended reach to the external flow (subcritical region).

The negative region of the original blade is suppressed by keeping only the useful portions. Figure 4a shows the effect of the inside blade length ratio l_1/W by fixing the tip length equals the original blade ($l_2/W = 1.125$). At the blade top, magnitudes of the C_t and C_a almost match with the original single blade and lower than the original at the inner portion. The tendency of C_t comes to be negative values at the bottom when increasing l_1/W. The positive inner length of $l_1/W = 0.75$ is employed to study the top length effect l_2/W and shown in Fig. 4b. The C_t and C_a of the increasing tip length are higher than the shorter length. The effect of the tip vortex is powerful for cutting the inner portion. However, the symmetrical

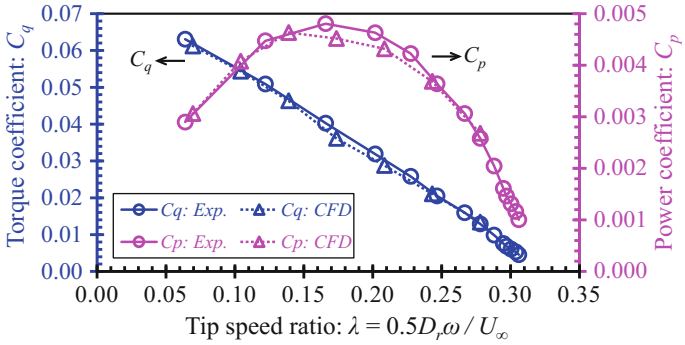

Fig. 5 Comparison between CFD results and experiment data for the $l_1/W = l_2/W = 1$ ($l = 3$ W)

distribution appears on the equally blade extension and the efficiency based on swept area is higher than the single cylinder blade system.

The equally blade extension $l_1/W = l_2/W = 1$ is selected to build for the wind tunnel investigation. The two cylinder-blades are fixed with a hub and a shaft which is connected to the torque meter 0.2 N m UMT II and the electrical brake HB0.5 N m. The torque T and the rotational speed ω of the rotor shaft are measured by the torque meter, while the electrical brake applies a load on the shaft for adjusting the ω. The experimental platform system (Fig. 1) is examined in a low turbulence intensity wind tunnel (0.6% at $U_\infty \geq 2$ m/s and 0.3% for $U_\infty \geq 11.2$ m/s) which has the test section of 0.32 m × 0.32 m × 1 m and the velocity range of 0.5–40 m/s. The ring-type anemometer is set upstream for measuring the U_∞. Both the CFD and experiment are tested for $U_\infty = 10$ m/s, the rotational speed is controlled and varied, and the predicting torque coefficient $C_q = T/0.5\rho R A_r {U_\infty}^2$ is used for comparison. Where $A_r = \pi({D_r}^2 - (D_r - 2l)^2)/4$ is the rotor swept area, $R = D/2$ is the radius of the ring. Power coefficient $C_p = T\omega/0.5\rho A_r {U_\infty}^3$ is estimated and reported in Fig. 5. The tendencies of the C_p and C_q against λ from both the CFD and experimental predictions correlate very well with a small difference. The torque is linearly decreased when increasing tip speed ratio, the maximum power coefficient $C_p \approx 0.005$ at around $\lambda = 0.15$–0.2 in both the experiment and calculation.

4 Conclusions

Flow around the simple single-cylinder blade LV-WT is investigated numerically, with a focus on the effective area of the blade to suppress the negative portions. The results are following:

1. The single cylinder blade, the flow visualization shows the mechanism of the steady lift force generation that is produced by the suction flow of the LV. The positive driving force is generated around the crossing area where is the LV

regime, and outlying regions are the subcritical flow that the negative driving force is produced.
2. The negative region is suppressed by keeping only the useful portions, but the driving force near both tip ends are lower than the original case due to the tip effect. The equally blade extension of $l_1 = l_2 = W$ is selected and built for the wind tunnel and computational investigations. The experimental and numerical predictions have a good agreement of the value and tendency. The effect of the free ends will be investigated in the future in order to increase the efficiency of the system.

Acknowledgements This work was supported by MEXT KAKENHI grant number JP16685247.

References

1. Bychkov NM, Dovgal AV, Kozlov VV (2007) Magnus wind turbines as an alternative to the blade ones. J Phys Conf Ser 75(012004):1–7
2. Schlichting H, Gersten K (2000) Boundary-layer theory, 8th edn. Springer, Berlin, Germany
3. Takahashi T, Yoshitake Y, Sakamoto K, Hemsuwan W (2016) An innovative wind/water turbine with circular propeller driven by longitudinal vortex. In Proceeding of the 15th WWEC2016 TOKYO conference, Japan. PS-A-5